Krauklis wave in a stack of alternating fluid-elastic layers

Valeri A. Korneev[1]

ABSTRACT

The Krauklis wave is a slow dispersive wave mode that propagates in a fluid layer bounded by elastic media. In a model of alternating fluid and elastic layers, two interface waves can exist at low frequencies: The first wave propagates mostly in the elastic layer and has little dispersion, while the second wave can have strong dispersion and propagates as a Krauklis wave for some parameter combinations. Analytical conditions predict appearance of the Krauklis wave for higher frequencies and low porosities. Interface-wave velocities depend on model porosity, which potentially can be used for fracture mapping.

INTRODUCTION

Propagation of waves in a system of fractures filled with fluid has been considered in many publications (Rytov, 1956; Brekhovskikh, 1980; Shoenberg, 1983, 1984; Molotkov, 2001; Gurevich, 2002; Ciz et al., 2006). When fractures are multiple, parallel, and thin, then two types of interface quasicompressional waves can propagate along the fracture surfaces: one is mostly associated with the elastic layers, the other with the fluid layers (Brekhovskikh, 1980). Molotkov (1988, 2001) has reported that not just two, but three different quasicompressional waves can propagate along a stack of fluid-filled fractures. Because such a statement contradicts previously obtained results, we must revisit the considered problem. In addition to this motivation, a high-amplitude dispersive fluid wave, which popagates along a single fluid layer, causes a special interest (Goloshubin et al., 1993, 1994; Korneev et al., 2009; Frehner and Schmalholz, 2010). This wave was first reported by Krauklis (1962)), who, in studying single fractures, found its analytical form and described its main properties, such as dominant polarization along the walls, high dispersion, and a propagation velocity going to zero at the zero frequency limit. Independently, Lloyd and Redwood (1965) and later Paillet and White (1982) found this wave numerically, as a root of the correspondent determinant for a linear system representing boundary conditions. Since then, many authors have reported on interesting properties of this slow fluid wave, including its high-amplitude and its central role in wave propagation within fractures (Ferrazzini and Aki, 1987; Groenenboom and Fokkema, 1998; Groenenboom and Falk, 2000, Ziatdinov, et al., 2006; Korneev, 2008; Korneev et al., 2009; Derov et al., 2009; Frehner and Schmalholz, 2010). Some authors (Bell and Fletcher, 2004; Elliott, 2007) suggest that these slow fluid waves play a key role in hearing physiology. In the literature, this wave is known by different names: "slow fluid wave" (Krauklis, 1962; Ferrazzini and Aki, 1987), "crack wave" (Chouet, 1986), "Stoneley wave" (Tang and Cheng, 1988), "Stoneley guided wave" (Korneev, 2008; Frehner and Schmalholz, 2010), "symmetric Lloyd-Redwood (SLR)" or "squirting wave" (Bell and Fletcher, 2004; Elliott, 2007).

Today, there is a growing consensus among the specialists (B. Kashtan, L. Molotkov, A. Bakulin, G. Maximov, G. Goloshubin, M. Frehner, and S. Nakagawa, personal communications, 2011) to name the slow fluid wave within a fracture after Pavel Krauklis, who found it first in 1962. Remarkably, Krauklis (1962) presented in his original paper an analytical solution for this wave for a model containing elastic halfspaces with different material properties, whereas up to now, researchers dealt with models that accounted just for the same material for both fracture walls. In 2008, Krauklis devoted numerous papers to slow waves, studying their propagation and attenuation in different models. In the following, I will use the term "Krauklis wave" for a slow dispersive wave that propagates in a fluid-saturated layer bounded by elastic media.

The Krauklis wave has been observed in the laboratory (Tang and Cheng, 1988; Hassan and Nagy, 1997), in field data during hydrofracturing (Ferrazzini et al., 1990), and in crosswell seismic (Goloshubin et al., 1994). Chouet (1996) suggested that low-frequency seismic tremors taking place before volcano eruptions can be explained by this wave propagating in magma conduits.

The natural questions are: Does the Krauklis wave exist in a layered fluid-elastic medium, and what are the conditions of its existence?

In this paper, I demonstrate that just two quasicompressional low-frequency waves can propagate along a stack of fluid-filled fractures. At the low-frequency limit, neither wave shows dispersion, and their propagation behavior depends on porosity. When the fractures are well-separated and the fluid fracture waves experience little interference, the second fluid wave propagates as a Krauklis wave.

THEORY

Consider an infinite model of alternating horizontal homogeneous layers (Figure 1), wherein a layer of the first kind ($j = 1$) has thickness h and consists of a nonviscous fluid, whereas the adjacent layers of the second kind ($j = 2$) are elastic and have thickness d. This model can be characterized by porosity $p = h/(h + d)$.

Derivation of the equation for finding the phase velocities V of waves propagating along the layers is presented in Appendix A (equation A-37). After substitution of some notations, this equation can be put in the form

$$\xi_1\left(\frac{(1-\alpha_{S2}^2/2)^2}{\xi_2}-\frac{1}{\chi_2}\right)-\frac{\rho_1\alpha_{S2}^2V^2}{4\mu_2}=0, \tag{1}$$

where

$$\xi_1=\tanh\left(\sqrt{1-\alpha_{P1}^2}\frac{\omega h}{2V}\right)\sqrt{1-\alpha_{P1}^2}, \tag{2}$$

$$\xi_2=-\tanh\left(\sqrt{1-\alpha_{P2}^2}\frac{\omega d}{2V}\right)\sqrt{1-\alpha_{P2}^2}, \tag{3}$$

$$\chi_2=-\tanh\left(\sqrt{1-\alpha_{S2}^2}\frac{\omega d}{2V}\right)/\sqrt{1-\alpha_{S2}^2}, \tag{4}$$

$$\alpha_{P1}=\frac{V}{V_{\mathrm{P1}}},\qquad \alpha_{P2}=\frac{V}{V_{\mathrm{P2}}}\qquad \alpha_{S2}=\frac{V}{V_{\mathrm{S2}}}, \tag{5}$$

where angular frequency is ω, fluid density is ρ_1, and shear modulus of the elastic walls is μ_2. No restrictions on parameter values were used for derivation of equation 1. Even when the radicals in equations 2, 3, and 4 become imaginary, all components of equation 1 remain real and do not depend on a sign choice for the radicals.

If the arguments x in all $\tanh(x)$ functions in equations 23, and 4 are small enough (thin layers) to allow the expansion

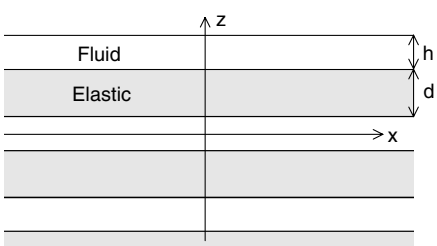

Figure 1. Model geometry of alternating fluid-elastic horizontal layers.

$$\tanh(\mathrm{x})\approx \mathrm{x} \tag{6}$$

then equation 1 becomes a square polynomial with respect to V^2

$$V^4\left(\frac{1}{V_{\mathrm{P2}}^2}+\frac{q}{4V_{\mathrm{S2}}^2}\right)-V^2\left(1+q\left(1-\gamma^2+\frac{V_{\mathrm{P1}}^2}{4V_{\mathrm{S2}}^2}\right)\right)+qV_{\mathrm{P1}}^2(1-\gamma^2)=0 \tag{7}$$

where

$$q=\frac{4}{V_{\mathrm{P1}}^2}\frac{\mu_2}{\rho_1}\frac{h}{d}=4\frac{\mu_2}{\lambda_1}\frac{p}{1-p}, \tag{8}$$

and the elastic velocities ratio is $\gamma = V_{\mathrm{S2}}/V_{\mathrm{P2}}$. Equation 7 has two real roots $\tilde{V}_1$ and $\tilde{V}_2$ corresponding to two possible waves. Note that equation 7 contains no frequency as a parameter and, therefore, its solutions represent nondispersive waves.

When $q \ll 1$, signifying a "small porosity" regime, then

$$V_1=\tilde{V}_1=V_{\mathrm{P2}}, \tag{9}$$

with P-velocity in the elastic medium, and

$$V_2=\tilde{V}_2=2\sqrt{\frac{\mu_2}{\rho_1}\frac{p}{1-p}(1-\gamma^2)}. \tag{10}$$

When $q \gg 1$, signifying a "large porosity" regime, then

$$V_1=\tilde{V}_1=V_{\mathrm{L}}\equiv 2\sqrt{(1-\gamma^2)}V_{\mathrm{S2}} \tag{11}$$

is the velocity of the symmetric Lamb wave (Lamb, 1917) in an isolated elastic slab, and

$$V_2=\tilde{V}_2=V_{\mathrm{P1}}, \tag{12}$$

is the velocity in the fluid.

Now, assume that the arguments of all $\tanh(x)$ functions in equations 2–4 are large enough to use the asymptotic form

$$\tanh(\mathrm{x})\approx\pm 1, \tag{13}$$

which, for example, can exist at high frequencies. Equation 1 now has the form

$$R+\frac{\rho_1V^4}{4\mu_2V_{\mathrm{S2}}^2\sqrt{1-\alpha_{P1}^2}}=0, \tag{14}$$

which is that of a Scholte wave equation (Scholte, 1942), where

$$R\equiv\frac{(1-\alpha_{S2}^2/2)^2}{\sqrt{1-\alpha_{P2}^2}}-\sqrt{1-\alpha_{S2}^2}. \tag{15}$$

Equation $R = 0$ (e.g., for vanishing fluid density) has two physical solutions in the form of Rayleigh waves (Malischewsky, 2004). Real parts of the square roots in the equations 14 and 15 should be chosen positive. Plus and minus signs give solutions correspondingly at the upper and lower layer interfaces. Neither Scholte waves (a real solution for equation 14) nor Rayleigh waves depend on

frequency, and thus propagate correspondingly with constant velocities V_{ST} and V_R

If the expansion 13 is valid for the functions in equations 3 and 4, and also we can apply the expansion 6 in equation 2 ("thin" fractures between "thick" elastic plates), then we obtain the dispersion equation for the Krauklis wave

$$(1-\alpha_{P1}^2)R + \frac{\rho_1 \alpha_{S2}^2 V^3}{2\mu_2 \omega h} = 0, \tag{16}$$

which has the solution (Krauklis, 1962; Korneev, 2008)

$$V_2 = V_K \equiv \left(\frac{\omega h \mu_2}{\rho_1}(1-\gamma^2)\right)^{\frac{1}{3}}. \tag{17}$$

Approximations 13 in equations 3 and 4 become satisfied when the arguments are approximately equal to two, and therefore the condition for existence of solution 17 is

$$\sqrt{1-\alpha_{S2}^2}\,\frac{\omega d}{2V_K} \approx \frac{\omega d}{2V_K} > 2. \tag{18}$$

The transition from the nondispersive solution 10 to the Krauklis wave takes place when

$$\frac{d}{4}\left(\frac{\omega^2 \rho_1}{h\mu_2(1-\gamma^2)}\right)^{\frac{1}{3}} \approx 1. \tag{19}$$

On the other hand, the condition 6 for equation 2 is approximately satisfied when

$$\frac{\omega h}{2V_K} \ll 1. \tag{20}$$

Numerical evaluations suggest that a transition corresponding to condition 20 occurs when

$$\frac{\omega h}{2V_K} \approx 0.1. \tag{21}$$

Conditions 18 and 20 signify that the Krauklis wave can exist only when $d \gg h$. At frequencies higher than those defined by condition 20, the Krauklis wave loses its dispersive properties when crossing the point where the condition 21 is satisfied, and then converts into a Scholte wave.

NUMERICAL RESULTS

The sets of material parameters used in the numerical examples below are shown in Table 1, with the water parameters used for fluid and the elastic layers represented by "fast" ($V_{S2} > V_{P1}$), and "slow" ($V_{S2} < V_{P1}$) materials. Equation 1 was used for finding exact solutions for velocities V_1 and V_2, using a numerical root search procedure. In the following figures, these velocities are plotted together with model velocities V_{P1}, V_{P2}, and V_{S2}, the Scholte wave solution V_{ST} of equation 14, the solutions $\tilde{V}_1$ and $\tilde{V}_2$ of equation 7, and with velocity V_K for the Krauklis wave from equation 17. The velocities V_1 and $\tilde{V}_1$ practically coincide for all cases. The points where conditions 19 and 21 become satisfied are marked by vertical arrows with the corresponding labels 1 and 2. Figure 2 shows the dependence of velocities on frequency for $h = 1$ mm and $d = 1$ m ($p \approx 10^{-3}$) for a fast elastic model. The same parameters were used for the slow elastic model shown in Figure 3. The fast model was also used for plotting the velocities as functions of model porosity (Figure 4) for a 100-Hz frequency, and the fixed spatial period $h + d = 1$ m. Figures 2, 3, and 4 do not show the higher modes appearing at high frequencies (e.g., see Coulouvrat et al., 1998), which are not a subject of this study.

DISCUSSION

For a wide range of parameters, the interface waves in the considered layered model have no dispersion at low frequencies. This might seem somewhat surprising because a single fluid layer exhibits very strong dispersion for a fluid wave in the form of the Krauklis wave. Physically, the Krauklis wave is interpreted as the interaction of the fluid mass and the elasticity of walls, described by the ratio μ_2/ρ_1 (equation 17), resulting from continuity of normal stress (equation A-15). For a single layer, the deformation of the walls is caused by the motion of fluid from one side of the elastic halfspace; however, in the case of the layered model, each elastic

Table 1. Material parameters for numerical examples.

Models	V_P (m/s)	V_S (m/s)	Density (Kg/m^3)
Water	1500	0	1000
Elastic fast	4000	2200	2700
Elastic slow	2000	1000	2700

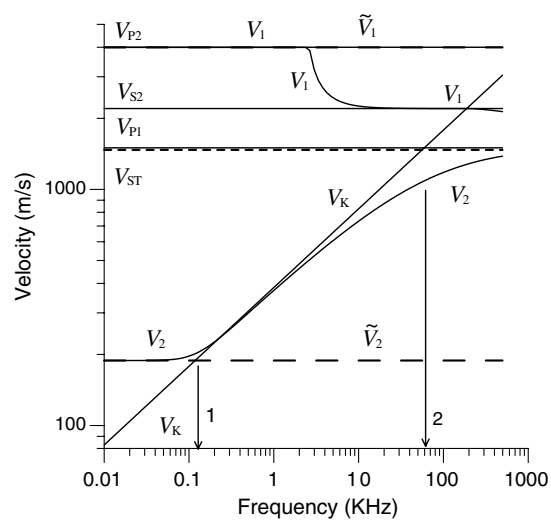

Figure 2. Phase velocities for the fast ($V_{S2} > V_{P1}$) elastic layers. Shown are: the exact solutions for velocities V_1 and V_2, model velocities V_{P1}, V_{P2}, and V_{S2}, Scholte wave solution V_{ST} of equation 14, solutions $\tilde{V}_1$ and $\tilde{V}_2$ of equation 7, and with velocity V_K for Krauklis wave from equation 17. The vertical arrows mark the points where the conditions 19 (arrow 1) and 21 (arrow 2) become satisfied. The higher modes with cutoff frequencies are not shown.

layer is subjected to the actions of symmetric forces from both sides. These forces compensate for each other, leaving a small contribution of elastic forces in the total stress. Krauklis waves appear in the layered model only when fluid layers are separated far enough when the interaction of these waves in the middle of elastic layers is negligibly small. Conditions 18 and 20 give the criteria for Krauklis waves to exist in the considered model and suggest that such waves can exist in real rock with preferential fracture orientation. Moreover, most fracture systems in nature exhibit a fractal character: they can be oriented arbitrarily and their thicknesses are also randomly distributed, leaving little room for perfect symmetry and self-compensation of fluid waves. It seems likely that the dispersive properties of Krauklis waves in rock fractures can be a rather common phenomenon.

In considering wave propagation problems, it is usually important to make the proper choice of signs before the radicals to ensure

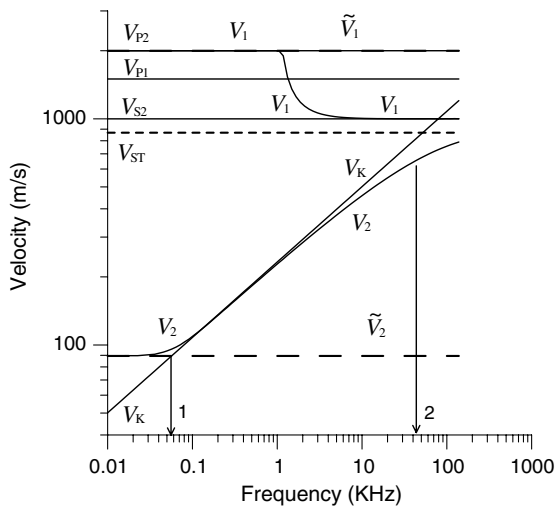

Figure 3. Phase velocities for the slow velocity model. Notations are the same as on Figure 2.

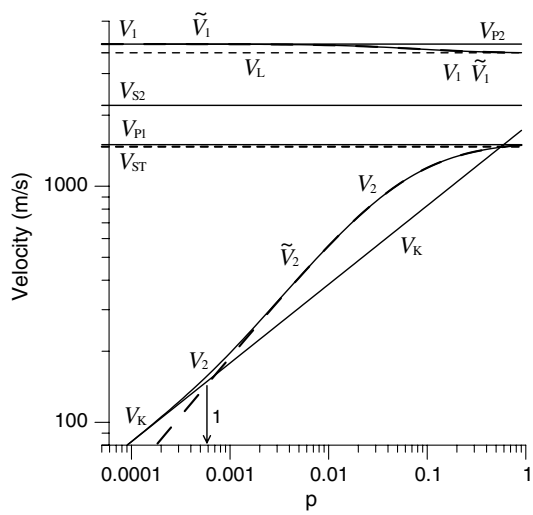

Figure 4. Phase velocities for the fast model as functions of model porosity p. Notations are the same as on Figure 2. Also shown Lamb wave velocity V_L (equation 11).

the physical meanings of the obtained solutions. However, in the considered problem for unbounded layered models, the choice of signs does not affect the solution. It can be readily seen that all the of equations 2, 3, and 4 do not depend on the radical sign and remain real even when any of radicals becomes purely imaginary. This fact reflects the infiniteness of the model in which wave energy has nowhere to leak to. Each layer loses the same amount of energy that it receives from its neighbors.

Velocity curves for the fast and slow waves (Figures 2 and 3) look rather similar. In both cases, the fluid wave flattens to a Scholte wave velocity at high frequencies. The main difference here appears in the value of V_{ST}. For the fast model, V_{ST} is slightly less than the fluid velocity V_{P1}, while for the slow model, it is slightly less than the shear velocity V_{S2} in the plate. Therefore, the real root of the Scholte equation is defined by the slowest velocity of the model.

The results of this study did not confirm the existence of the three quasicompressional waves reported by Molotkov (1988, 2001). Similar to Brekhovskikh (1980), I have found just two waves, coinciding with wave 1 and wave 3 in Molotkov's notation. His wave 2 is a symmetrical Lamb wave, which I obtain as an asymptotic solution for the first (fast) wave in the high porosity limit. The difference in results is likely caused by a difference in methods for obtaining the solutions. As a starting point, I used the exact solution in the form of equation A-14. Then I used thin layer assumptions to obtain the quadratic polynomial (equation 7). Molotkov (2001, page 247) used thin layer limits ($h \to 0$ and $d \to 0$) at the stage of averaging the equations of motion. In doing so, he ignores the boundary condition for the tangential stress component, arguing that after applying the limits a computation of derivatives $\partial u_x/\partial z$ becomes undefined because u_x is a discontinuous function across the interface (L. A. Molotkov, personal communication, 2011). I find this argument hard to justify, especially because his results are not fully supported by the exact formulation used in this paper.

Both of the waves propagating along the stack of fractures show a strong dependence on the porosity. This property might indicate the presence of fractures and might possibly be used for evaluation and mapping of fractures. In low-density fracture zones where conditions 18 and 20 are satisfied, the dispersive Krauklis wave can possibly contribute additional information about fracture properties.

CONCLUSIONS

An alternating fluid-elastic layered model is capable of carrying two types of quasicompressional interface waves at low frequencies. The first wave propagates mostly in elastic layers and has little dispersion. The second (fluid) wave can, for some parameter combinations, exhibit strong dispersion when propagating as a Krauklis wave. Such a mode of propagation is even more likely in real fractured rock with a random fracture orientation.

ACKNOWLEDGMENTS

This work was supported by the Research Partnership to Secure Energy for America (RPSEA) through the director, Office of Science, Office of Basic Energy Sciences, GEO-SEQ project for the Assistant Secretary for Fossil Energy, Office of Coal and Power Systems through the National Energy Technology Laboratory of the U.S. Department of Energy under contract No. DE-AC02-05CH11231. Boris Kashtan was the first to suggest naming the slow

fluid wave after Pavel V. Krauklis. The author thanks Lev A. Molotkov for helpful discussions. Marcel Frehner, Karel van Dalen, and an anonymous reviewer have made many important comments.

APPENDIX A

DERIVATION OF DISPERSION EQUATION

Consider a horizontally layered infinite model of alternating homogeneous layers (Figure 1) in which the layers of the first kind ($j = 1$) have thickness h and consist of nonviscous fluid, while the adjacent layers of the second kind ($j = 2$) are elastic and have thicknesses d. Layers are aligned along the OX axis of the x spatial coordinate. The OZ axis is orthogonal to the layer interfaces with the origin in the middle of one of the layers of the first kind. We are interested in waves propagating along the layer surfaces following an analogous derivation originally used by Rytov (1956) for a model with two alternating elastic layers. The time t dependence of the fields is taken in the form $\exp(-i\omega t)$, with angular frequency ω, and $i = \sqrt{-1}$.

Displacements $\mathbf{u}^{(j)}$ in both layers $j = 1$, two obey the equations of motion

$$(\lambda_j + \mu_j)\nabla\nabla \cdot \mathbf{u}^{(j)} + \mu_j \Delta \mathbf{u}^{(j)} + \omega^2 \rho_j \mathbf{u}^{(j)} = 0 \tag{A-1}$$

and can be represented as the sum

$$\mathbf{u}^{(j)} = \mathbf{u}_P^{(j)} + \mathbf{u}_S^{(j)} \tag{A-2}$$

where $\mathbf{u}_P^{(j)}$ and $\mathbf{u}_S^{(j)}$ are compressional and shear components, respectively. These components obey the equations

$$\nabla \times \mathbf{u}_P^{(j)} = 0, \qquad \nabla \cdot \mathbf{u}_S^{(j)} = 0, \tag{A-3}$$

and relate to potentials φ_j and ψ_j through the following equations

$$\mathbf{u}_P^{(j)} = \nabla \varphi_j, \tag{A-4}$$

$$\mathbf{u}_S^{(j)} = \nabla \times (\psi_j \mathbf{y}_1), \tag{A-5}$$

where the unit vector along OY axis $\mathbf{y}_1$ is used. The potentials obey the equations

$$\Delta \varphi_j + \frac{\omega^2}{V_{\mathrm{P}j}^2} \varphi_j = 0 \tag{A-6}$$

$$\Delta \psi_j + \frac{\omega^2}{V_{\mathrm{S}j}^2} \psi_j = 0 \tag{A-7}$$

describing the longitudinal (P-) waves with velocities

$$V_{\mathrm{P}j} = \sqrt{\frac{\lambda_j + 2\mu_j}{\rho_j}} \tag{A-8}$$

and a shear (S-) waves with velocities

$$V_{\mathrm{S}j} = \sqrt{\frac{\mu_j}{\rho_j}}, \tag{A-9}$$

expressed through Lame constants λ_j, μ_j and density ρ_j ($j = 1, 2$). For the (fluid) layers of the first kind $\mu_1 = 0$, and correspondently $\psi_1 = 0$.

We consider the symmetrical wave modes propagating along the interfaces with the wavenumbers $k_x = \omega/V$, where V is propagation phase velocity. In such a case, the potentials have the forms

$$\varphi_1 = A_1 (e^{k_x \sqrt{1-\alpha_{P1}^2}(z+nl)} + e^{-k_x \sqrt{1-\alpha_{P1}^2}(z+nl)}) e^{\mathrm{i}k_x x}, \tag{A-10}$$

for the layers of the first kind, and

$$\varphi_2 = A_2 (e^{k_x \sqrt{1-\alpha_{P2}^2}(z+nl-l2)} + e^{-k_x \sqrt{1-\alpha_{P2}^2}(z+nl-l2)}) e^{\mathrm{i}k_x x}, \tag{A-11}$$

$$\psi_2 = B_2 (e^{k_x \sqrt{1-\alpha_{S2}^2}(z+nl-l/2)} - e^{-k_x \sqrt{1-\alpha_{S2}^2}(z+nl-l/2)}) e^{\mathrm{i}k_x x} \tag{A-12}$$

for the layers of the second kind, where $n = 0, \pm 1, \pm 2, \ldots$ is an index numerating of the interfaces, and $l = h + d$ is the spatial period of the model. In equations A-10, A-11, and A-12 we used the notations

$$\alpha_{Pj} = \frac{\omega}{k_x V_{\mathrm{P}j}} = \frac{V}{V_{\mathrm{P}j}}, \quad \alpha_{S2} = \frac{\omega}{k_x V_{\mathrm{S}2}} = \frac{V}{V_{\mathrm{S}2}}, \quad (j = 1, 2), \tag{A-13}$$

and A_j and B_2 are constants determined from satisfying the boundary conditions

$$u_z^{(1)} = u_z^{(2)}, \tag{A-14}$$

$$t_{zz}^{(1)} = t_{zz}^{(2)}, \tag{A-15}$$

$$t_{xz}^{(2)} = 0, \tag{A-16}$$

requiring continuity of normal component $u_z^{(j)}$ of displacement field, continuity of normal component for stress $t_{zz}^{(j)}$, and free surface condition for horizontal stress component $t_{zx}^{(2)}$. Expressions for the fields from equations A-14, A-15, and A-16 have the forms

$$u_z^{(j)} = \frac{\partial \varphi_j}{\partial z} + \frac{\partial \psi_j}{\partial x}, \tag{A-17}$$

$$\tau_{xz}^{(j)} = \mu_j \left(\frac{\partial u_x^{(j)}}{\partial z} + \frac{\partial u_z^{(j)}}{\partial x} \right), \tag{A-18}$$

$$\tau_{zz}^{(j)} = (\lambda_j + 2\mu_j) \nabla \cdot \mathbf{u}^{(j)} - 2\mu_j \frac{\partial u_x^{(j)}}{\partial x}. \tag{A-19}$$

With such choice of the fields, if we satisfy boundary conditions for n = 0 (the first interface at $z = h/2$), these conditions will be automatically satisfied at all other interfaces.

Introducing the notations

$$\varsigma^-(\alpha_{P1}) \equiv A_1(e^{k_x\sqrt{1-\alpha_{P1}^2}\frac{h}{2}} - e^{-k_x\sqrt{1-\alpha_{P1}^2}\frac{h}{2}}), \tag{A-20}$$

$$\varsigma^-(\alpha_{P2}) \equiv A_2(e^{-k_x\sqrt{1-\alpha_{P2}^2}\frac{d}{2}} - e^{k_x\sqrt{1-\alpha_{P2}^2}\frac{d}{2}}), \tag{A-21}$$

$$\varsigma^-(\alpha_{S2}) \equiv B_2(e^{-k_x\sqrt{1-\alpha_{S2}^2}\frac{d}{2}} - e^{k_x\sqrt{1-\alpha_{S2}^2}\frac{d}{2}}), \tag{A-22}$$

$$\varsigma^+(\alpha_{P1}) \equiv A_1(e^{k_x\sqrt{1-\alpha_{P1}^2}\frac{h}{2}} + e^{-k_x\sqrt{1-\alpha_{P1}^2}\frac{h}{2}}), \tag{A-23}$$

$$\varsigma^+(\alpha_{P2}) \equiv A_2(e^{-k_x\sqrt{1-\alpha_{P2}^2}\frac{d}{2}} + e^{k_x\sqrt{1-\alpha_{P2}^2}\frac{d}{2}}), \tag{A-24}$$

$$\varsigma^+(\alpha_{S2}) \equiv B_2(e^{-k_x\sqrt{1-\alpha_{S2}^2}\frac{d}{2}} + e^{k_x\sqrt{1-\alpha_{S2}^2}\frac{d}{2}}). \tag{A-25}$$

Expressions for boundary conditions (after dropping factor $e^{ik_x x}$) have the forms

$$u_z^{(1)} = k_x\sqrt{1-\alpha_{P1}^2}A_1\varsigma^-(\alpha_{P1}), \tag{A-26}$$

$$u_z^{(2)} = k_x\left(\sqrt{1-\alpha_{P2}^2}A_2\varsigma^-(\alpha_{P2}) + iB_2\varsigma^-(\alpha_{S2})\right), \tag{A-27}$$

$$\tau_{zx}^{(2)} = \mu_2 k_x^2\left(2i\sqrt{1-\alpha_{P2}^2}A_2\varsigma^-(\alpha_{P2}) - (2-\alpha_{S2}^2)B_2\varsigma^-(\alpha_{S2})\right), \tag{A-28}$$

$$\tau_{zz}^{(1)} = -\rho_1 V^2 k_x^2 A_1\varsigma^+(\alpha_{P1}), \tag{A-29}$$

$$\tau_{zz}^{(2)} = 2\mu_2\left(1-\frac{\alpha_{S2}^2}{2}\right)k_x^2 A_2\varsigma^+(\alpha_{P2}) + 2i\mu_2\sqrt{1-\alpha_{S2}^2}k_x^2 B_2\varsigma^+(\alpha_{S2}). \tag{A-30}$$

Velocities of the waves propagating along the interfaces of the model are the solutions of the equation

$$\begin{vmatrix} \sqrt{1-\alpha_{P1}^2}\varsigma^-(\alpha_{P1}) & \sqrt{1-\alpha_{P2}^2}\varsigma^-(\alpha_{P2}) & \varsigma^-(\alpha_{S2}) \\ -\rho_1 V^2\varsigma^+(\alpha_{P1}) & 2\mu_2\left(1-\frac{\alpha_{S2}^2}{2}\right)\varsigma^+(\alpha_{P2}) & 2\mu_2\sqrt{1-\alpha_{S2}^2}\varsigma^+(\alpha_{S2}) \\ 0 & \sqrt{1-\alpha_{P2}^2}\varsigma^-(\alpha_{P2}) & (1-\alpha_{S2}^2/2)\varsigma^-(\alpha_{S2}) \end{vmatrix} = 0, \tag{A-31}$$

resulting from boundary conditions.

Introducing notations

$$\xi_1 = \tanh\left(\sqrt{1-\alpha_{P1}^2}\frac{k_x h}{2}\right)\sqrt{1-\alpha_{P1}^2}, \tag{A-32}$$

$$\xi_2 = -\tanh\left(\sqrt{1-\alpha_{P2}^2}\frac{k_x d}{2}\right)\sqrt{1-\alpha_{P2}^2}, \tag{A-33}$$

$$\chi_2 = -\tanh\left(\sqrt{1-\alpha_{S2}^2}\frac{k_x d}{2}\right)/\sqrt{1-\alpha_{S2}^2}, \tag{A-34}$$

$$a = \frac{\rho_1 V^2}{2\mu_2}, \qquad b = 1-\frac{\alpha_{S2}^2}{2}, \tag{A-35}$$

we get

$$\begin{vmatrix} \xi_1 & \xi_2 & \chi_2 \\ -a & b & 1 \\ 0 & \xi_2 & b\chi_2 \end{vmatrix} = 0, \tag{A-36}$$

or

$$\xi_1(b^2\chi_2 - \xi_2) + a\xi_2\chi_2(b-1) = 0. \tag{A-37}$$

REFERENCES

Bell, A., and N. H. Fletcher, 2004, The cochlear amplifier as a standing wave: "Squirting" waves between rows of outer hair cells?: Journal of the Acoustic Society of America, **116**, no. 2, 1016–1024, doi: 10.1121/1.1766053.

Brekhovskikh, L. M., 1980, Waves in layered media, 2nd ed.: Academic Press.

Chouet, B., 1986, Dynamics of a fluid-driven crack in three dimensions by the finite-difference method: Journal of Geophysical Research, **91**, 13967–13992, doi: 10.1029/JB091iB14p13967.

Ciz, R., E. H. Saenger, and B. Gurevich, 2006, Pore scale numerical modeling of elastic wave dispersion and attenuation in periodic systems of alternating solid and viscous fluid layers: Journal of the Acoustic Society of America, **120**, no. 2, 642–648, doi: 10.1121/1.2216687.

Coulouvrat, F., M. Rousseau, O. Lenoir, and J. Izbicki, 1998, Lamb-type waves in a symmetric solid-fluid-solid trilayer: Acustica, **84**, no. 1, 12–20.

Derov, A., G. Maximov, M. Lazarkov, B. Kashtan, and A. Bakulin, 2009, Tube waves from a horizontal fluid-filled fracture of a finite radius: 79th Annual International Meeting, SEG, Expanded Abstracts, 4115–4119.

Elliott, S. J., 2007, Wave propagation in a constrained fluid layer bounded by an elastic half-space and its relevance in cochlear micromechanics: Journal of Sound and Vibration, **305**, no. 4–5, 918–924, doi: 10.1016/j.jsv.2007.04.040.

Ferrazzini, V., and K. Aki, 1987, Slow waves trapped in a fluid-filled infinite crack: Implications for volcanic tremor: Journal of Geophysical Research, **92**, 9215–9223, doi: 10.1029/JB092iB09p09215.

Ferrazzini, V., B. Chouet, M. Fehler, and K. Aki, 1990, Quantitative analysis of long-period events recorded during hydrofracture experiments at Fenton Hill, New Mexico: Implications for volcanic tremor: Journal of Geophysical Research B, **95**, no. B13, 21871–21884.

Frehner, M., and S. Schmalholz, 2010, Finite-element simulations of Stoneley guided wave reflection and scattering at the tips of fluid-filled fractures: Geophysics, **75**, no. 2, T23–T36, doi: 10.1190/1.3340361.

Goloshubin, G. M., P. V. Krauklis, L. A. Molotkov, and H. B. Helle, 1993, Slow wave in oil-saturated layer: 55th Annual Conference and Exhibition, EAGE.

Goloshubin, G. M., P. V. Krauklis, L. A. Molotkov, and H. B. Helle, 1994, Slow wave phenomenon at seismic frequencies: 63rd Annual International Meeting, SEG, Expanded Abstracts, 809–811.

Groenenboom, J., and J. Falk, 2000, Scattering by hydraulic fractures: Finite-difference modeling and laboratory data: Geophysics, **65**, 612–622, doi: 10.1190/1.1444757.

Groenenboom, J., and J. T. Fokkema, 1998, Guided waves along hydraulic fractures: 67th Annual International Meeting, SEG, Expanded Abstracts, 1632–1635.

Gurevich, B., 2002, Effect of fluid viscosity on elastic wave attenuation in porous rocks: Geophysics, **67**, 264–270, 10.1190/1.1451798.

Hassan, W., and P. E. Nagy, 1997, On the low-frequency oscillation of a fluid layer between two elastic plates: Journal of the Acoustic Society of America, **102**, no. 6, 3343–3348, doi: 10.1121/1.419576.

Korneev, V. A., 2008, Slow waves in fractures filled with viscous fluid: Geophysics, **73**, no. 1, N1–N7, doi: 10.1190/1.2802174.
Korneev, V. A., A. Ponomarenko, and B. Kashtan, 2009, Stoneley guided waves: What is missing in Biot's theory?: Proceedings of the Fourth Biot Conference on Poromechanics: DEStech Publication Inc., 706–711.
Krauklis, P. V., 1962, About some low frequency oscillations of a liquid layer in elastic medium: PMM, **26**, no. 6, 1111–1115 (in Russian).
Lamb, H., 1917, On waves in an elastic plate: Proceedings of the Royal Society of London, Series A: Mathematical, Physical and Engineering Sciences, **A93**, 114–128, doi: 10.1098/rspa.1917.0008.
Lloyd, P., and M. Redwood, 1965, Wave propagation in a layered plate composed of two solids with perfect contact, slip, or a fluid layer at their interface: Acustica, **16**, 224–232.
Malischewsky, P. G., 2004, A note on Rayleigh-wave velocities as a function of the material parameters: Geofisica internacional: Revista de la Union Geofisica Mexicana auspiciada por el Instituto de Geofisica de la Universidad Nacional Autonoma de Mexico, **43**, no. 3, 507–509.
Molotkov, L. A., 1988, Peculiarities of wave propagation in layered models of fractured media: Proceedings of Saint Petersburg Branch of Steklov Mathematical Institute (in Russian), **173**, no. 18, Mathematical Problems of Wave propagation Theory, 123–133 (English translation in Journal of Soviet Mathematics, 1991, **55**, no. 3).
Molotkov, L. A., 2001, Study of wave propagation in porous and fractured media based on effective modes of Biot's and fractured media (In Russian): Nauka, 384.
Paillet, F. L., and J. E. White, 1982, Acoustic models of propagation in the borehole and their relationship to rock properties: Geophysics, **47**, 1215–1228, doi: 10.1190/1.1441384.
Rytov, S. M., 1956, Acoustical properties of a thinly laminated medium: Soviet Physics Acoustics, **2**, 68–80.
Schoenberg, M., 1983, Wave propagation in a finely laminated periodic elastoacoustic medium: Applied Physics Letters, **42**, 350–352, doi: 10.1063/1.93929.
Schoenberg, M., 1984, Wave propagation in alternating fluid/solid layers: Wave Motion, **6**, 303–320, doi: 10.1016/0165-2125(84)90033-7.
Scholte, J. G., 1942, On the Stoneley wave equation: Proceedings Nederlanse Akademic van Wetenschappen, **45**, 159–164.
Tang, X. M., and C. H. Cheng, 1988, Wave propagation in a fluid-filled fracture — An experimental study: Geophysical Research Letters, **15**, 1463–1466, doi: 10.1029/GL015i013p01463.
Ziatdinov, S., A. Bakulin, and B. Kashtan, 2006, Tube waves from a horizontal fluid-filled fracture of a finite radius: 76th Annual International Meeting, SEG, Expanded Abstracts, 369–372.

DISCLAIMER

This document was prepared as an account of work sponsored by the United States Government. While this document is believed to contain correct information, neither the United States Government nor any agency thereof, nor The Regents of the University of California, nor any of their employees, makes any warranty, express or implied, or assumes any legal responsibility for the accuracy, completeness, or usefulness of any information, apparatus, product, or process disclosed, or represents that its use would not infringe privately owned rights. Reference herein to any specific commercial product, process, or service by its trade name, trademark, manufacturer, or otherwise, does not necessarily constitute or imply its endorsement, recommendation, or favoring by the United States Government or any agency thereof, or The Regents of the University of California. The views and opinions of authors expressed herein do not necessarily state or reflect those of the United States Government or any agency thereof or The Regents of the University of California.

Ernest Orlando Lawrence Berkeley National Laboratory is an equal opportunity employer.